Soil thermal properties and heat transfer processes near Ny-Ålesund, northwestern Spitsbergen, Svalbard

JAAKKO PUTKONEN

Putkonen, J. 1998: Soil thermal properties and heat transfer processes near Ny-Ålesund, northwestern Spitsbergen, Svalbard. *Polar Research 17(2)*, 165–179.

The annually thawing active layer of permafrost is central to considerations of climate change consequences in arctic areas and interpretations of deep permafrost temperatures that constitute an exceptional archive of past climate change. Moreover, a sound understanding of the thermal regime of the active layer is of great interest, because all chemical, biological and physical processes are concentrated there. The author studied this layer by examining the soil physical properties and heat transfer processes that dictate soil temperatures for an arctic desert site in northwestern Spitsbergen. A wide array of soil physical properties based on field observations and laboratory measurements were defined. These include mineralogy, grain size distribution, local regolith thickness, porosity, density, typical soil moisture profile, heat capacity and thermal conductivity. Heat transfer processes were studied through modeling of soil temperatures. The heat transfer model accounted for much of the observed soil thermal regime. It was found that thermal conduction, phase change of soil water at 0°C, and changes in unfrozen water content are the primary thermal processes that explain the observed soil temperatures in this field site. Melt-water infiltration, which is often overlooked in the energy budget, causes abrupt warming events and delivers considerable energy to the soil in late spring. An increase in frequency or magnitude of infiltration events could mimic simple spring time surface warming. Advection of ground water and soil internal evaporation were found to be generally unimportant at the site studied.

Jaakko Putkonen, Quaternary Research Center, MS 351360, University of Washington, Seattle, WA 98195, U.S.A.

Introduction

Permafrost underlies approximately 25% of the world's land surface and is widespread in high latitude and altitude regions (Judge & Pilon 1983). Although climate warming is somewhat subdued when the effects of sulfate aerosol are included (Meehl. et al. 1996; Santer et al. 1995), the widely discussed models for contemporary greenhouse-induced climate change generally predict that warming will be greatest in high latitude regions (Budyko & Izrael 1987; Maxwell & Barrie 1989; Roots 1989; but see Kahl et al. 1993; Walsh 1993; IPCC 1996). This leads to the important expectation that current and impending climate change will alter the surface energy balance, the soil temperature and, hence, the distribution of permafrost (Nelson & Anisimov 1993; Riseborough & Smith 1993).

The specific effects of macro-scale climate change on permafrost are not likely to be simple because the interactions between climate, microclimate, surface and ground thermal conditions are complex (Putkonen in press). Nevertheless, theoretical considerations suggest that relatively rapid changes may occur in the active layer depth, defined as the depth of summer thaw, and in the distribution of warm permafrost near its southern limit. Changes in the depth of the active layer have diverse and far-reaching implications because practically all hydrologic, geomorphic, pedologic, chemical, and biological processes are sharply focused in this surface layer.

The anticipated increase in active layer depth would have direct societal consequences. Frost heave and differential thaw settlement would result in a significant increase of damage to houses, roads, airports and other structures, as well as raise the maintenance costs of these. Farming would be hindered because of thermokarst formation. An increase in the active layer depth would increase the incidence of slope stability problems (Permafrost Research, p. 15, 1983; Judge & Pilon 1983). Regions far beyond permafrost areas would also be influenced because greenhouse warming would be exacerbated

by the release of carbon dioxide and methane, currently stored in permafrost, to the atmosphere (Oechel et al. 1993).

In contrast with the upper boundary of permafrost, which is defined by the depth of summer thaw, changes in the position of the lower boundary of permafrost will generally be unimportant for thousands of years to come because of the slow conductive transfer of heat over typical length scales of hundreds of metres (Osterkamp & Gosink 1991). A virtue of this slow thermal response is that a direct archive of climatic events over the last centuries lingers in permafrost temperatures.

In the presence of a changing climate, therefore, permafrost can play at least three important roles: (1) a recorder of shallow ground temperature stored in deep permafrost; (2) an agent of environmental changes that affects landscapes and land-ocean and land-atmosphere interactions as well as ecological and human communities; and (3) an amplifier of further climate change (Nelson et al. 1993).

Fig. 1. Location map of Svalbard showing the field area.

Background

This work examines the factors that define the thermal regime of the soil in a permafrost area in an attempt to gain a better understanding of the 'complex and poorly understood regions (active layer, snow pack and boundary layer) through which the two temperatures [*permafrost and air temperature*] are coupled' (Lachenbruch & Marshall 1986). The focus is on the soil thermal properties and heat transfer processes that control the net energy budget of high latitude soils today. The work is motivated by the interest in improving the interpretation of the records of past soil temperatures and the assessment of the effects of upcoming climate change on the thermal regime of the active layer and permafrost.

The response of the soil energy budget to changes in environmental factors depends on heat transfer through the snow/soil system. This is modeled as conduction with latent heat transfers accompanying phase changes (equation 1).

Several aspects of this problem have been studied previously, including effects of snow cover on soil heat flow (Goodrich 1982; Sturm et al. 1995), soil heat flow in wet arctic tundra (Romanovski & Osterkamp 1995; Hinkel & Outcalt 1994; Kane et al. 1991), soil and snow surface heat transfer (Weller & Holmgren 1974) and rain-on-snow events (Woo & Heron 1981). However, all researchers except Woo (1981) have focused on relatively wet arctic or alpine tundra areas where the soil is covered by a substantial mat of organic material. This leaves the soil thermal regime of the vast high arctic region, which is sparsely vegetated and relatively dry, largely uncharacterised.

The work presented here is guided by data from a relatively dry arctic desert site (latitude 78°57′29N, longitude 12°27′42E), Brøggerhalvøya in western Spitsbergen, 10 km NW from Ny-Ålesund (Figs. 1, 2 and 3). Here the influence of plants, including thermal insulation and transpiration, is negligible. Completely void of vegetation, the surface of this site quickly dries up after summer storms, although the ground water table is not far from the surface throughout the summer (typically less than 0.5 metres). The relatively warm mean winter air temperature (mean of coldest month, February, is −14.6°C) permits examination of latent heat effects and other non-conductive soil heat transfer processes that are much less evident at lower temperatures. For a description of the field site, see Hallet & Prestrud (1986).

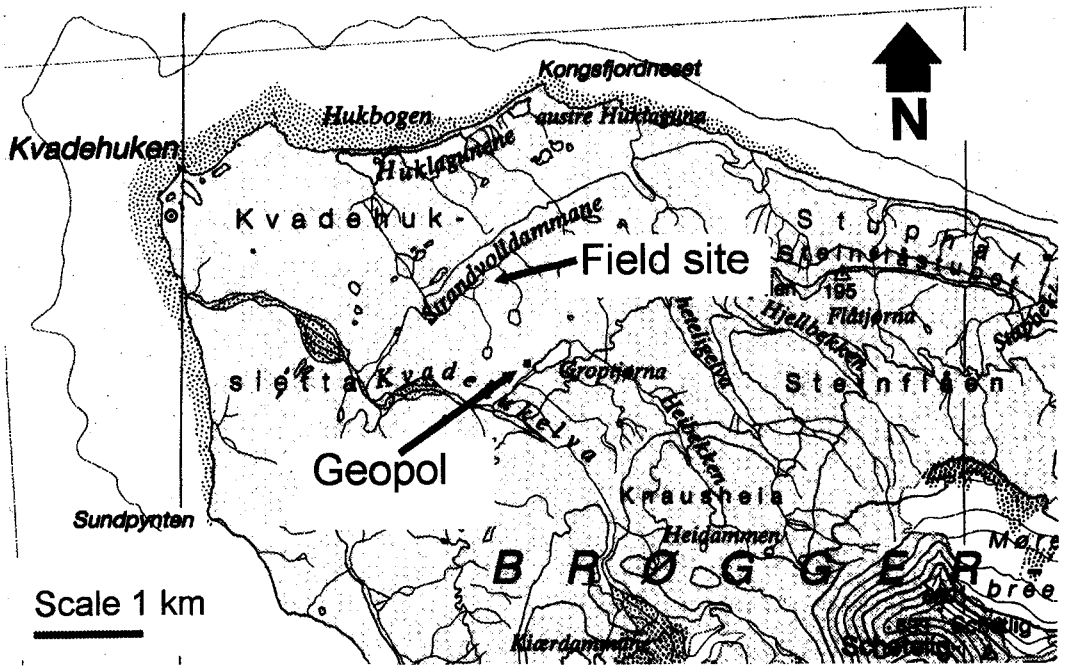

Fig. 2. Detailed map of the field area showing the field site, Geopol and Kvadehukelva (Modified from Norsk Polarinstitutt topographic map: Svalbard 1:100,000 Sheet A7 Kongsfjorden 1990).

The objectives of the study are to determine the soil thermal properties, heat transfer processes and develop a thermal model of soil surface heat flow under atmospheric forcing. This model is tested, validated and calibrated using soil temperature and micrometeorological data from a field site in western Spitsbergen.

The first part of this paper focuses on measurements and analysis of thermal processes in the active layer. Two issues are then examined: (1) the importance of vapor advection and associated phase changes in the soil as heat transfer processes during the summer and fall freeze up at this site, as suggested by Hinkel & Outcalt (1993) based on their studies in Alaska; (2) how modeling of heat conduction is affected by the use of field-monitored spatial and temporal variation in soil thermal properties. These properties vary in concert with moisture content and phase changes.

Fig. 3. Fenced field site in Kvadehuken.

Data

A program of automated soil temperature recordings was initiated in the summer of 1984 at a patterned, ground field site described by Hallet & Prestrud (1986). Thermistors were placed approximately 0.1 m apart in an epoxy-filled PVC rod (18 mm outside diameter) and buried in the centre of a fine-grained domain of a sorted circle 1.14 m below the ground surface. The thermistors were linked to a digital microprocessor; the frequency of measurements varied from 1–24/day. The resolution of the thermistors is 0.004°C,

and the accuracy is estimated to be 0.02°C near 0°C. Complementary recordings of frost heave and pore pressure were also available. Soil samples were collected to determine mineralogy, moisture content, thermal and hydraulic conductivity, and bulk density in the laboratory. During the summer of 1991 additional sensors were installed, two soil heat flow transducers (Radiation and Energy Balance Systems, Inc. (REBS), HFT-3, accuracy 0.1 W m^{-2}, 0.1 m and 0.2 m below surface). In addition, a thermal conductivity probe was installed 0.1 m below surface (Soiltronics, model TC2, accuracy ±5% (Shiozawa & Campbell 1990)).

Three relatively uninterrupted periods of data were used in the analyses: one year beginning in September 1985 to model a complete annual cycle, and the 1991 and 1992 summers to examine higher frequency events more closely. In light of standard meteorological observations, the September 1985–August 1986 period was average. Mean annual air temperature was −6.6°C, 0.4°C colder than the long term (1975–1990) mean, but well within the mean variability (σ = 1.3°C). Annual precipitation was 17% larger than long term mean (372 mm); however, the number of rain-on-snow events was less (3) than average (5.5). During the summer of 1991, the mean air temperature for July–August in Ny-Ålesund was 4.7°C, which is 0.2°C colder than the long-term mean. Overall, the reference periods are close to long-term averages.

Active layer thermal modeling

Modeling soil thermal regime

Good insight into the thermal regime of a laterally uniform soil can be gained using the general one-dimensional thermal diffusion equation with phase change (1).

$$\rho c \frac{\partial T}{\partial t} = \frac{\partial\left(k\frac{\partial T}{\partial z}\right)}{\partial z} + \frac{L_f \rho_w}{V_u}\frac{\partial V_f}{\partial t} = \frac{\partial k}{\partial z}\frac{\partial T}{\partial z} + k\frac{\partial^2 T}{\partial z^2} + \frac{L_f \rho_w}{V_u}\frac{\partial V_f}{\partial t} \quad (1)$$

Where T is temperature [°C], t is time [s], ρc is the soil heat capacity [J m^{-3} K^{-1}], k is soil thermal conductivity [W m^{-1} K^{-1}], z is depth [m], V_u is unit volume [1 m^3], L_f is latent heat of fusion of ice [J kg^{-1}], ρ_w is density of water [kg m^{-3}], V_f is volume of ice [m^3].

Physically this means that the time rate of temperature change is related to thermal conductivity and temperature gradient both above and below the level of interest and the rate of ice formation within the soil. The term for ice formation integrates both phase change at 0°C and the progressive freezing of unfrozen water as temperatures decrease below 0°C.

Measured soil temperatures were compared to temperatures calculated using an explicit finite difference approximation of equation (1) with two boundary conditions (for details of the discretisation process see Appendix A): the measured surface temperature and the temperature at 15 m, which was assumed fixed at −4.0°C. This basal temperature is the mean annual soil temperature at the lowest measurement level (1.14 m) corrected by 0.375°C to account for the geothermal gradient (using an average continental geothermal gradient of 25°C/1000 m for 14 m). This 15 m temperature corresponds closely to measurements obtained in comparable settings elsewhere in Spitsbergen. These borehole measurements in Ny-Ålesund, Longyearbyen and Sveagruva reveal temperatures between −3 to −7°C at 10–20 m (Liestøl 1975; Gregersen & Eidsmoen 1988). The depth to bedrock and the thermal properties of bedrock are estimated from observations and from analysed samples (see sections below).

Soil physical properties

Quantitative consideration of the soil thermal regime requires that the heat capacity and thermal conductivity of the soil be specified realistically. These thermal parameters depend on soil mineralogy, porosity and moisture content, as summarised in Table 1. These parameters commonly vary with depth and time because they are related to soil moisture content which also tends to vary in natural soils. Therefore, detailed thermal analysis essentially requires continuous in situ measurements of thermal properties.

Mineralogy, grain size and regolith thickness

The soil, comprising much of the fine-grained centres of sorted circles where the temperature data of interest were obtained, is a silt loam (Mann et al. 1986; Løvlie & Putkonen 1996). It contains considerable gravel, averaging 58.5% by weight, and ranging from 23–82% (pers. comm. B. Hallet 1995). Mineralogically, the soil resem-

Table 1. Physical characteristics of soil minerals.

Mineral type	Mineral density[1] [kg m^{-3}]	Volume fraction	Heat capacity[2] [J kg^{-1} K^{-1}]	Thermal conductivity [W m^{-1} K^{-1}][1][2]
Dolomite	2830	0.8	813	4.98
Calcite	2700	0.1	795	3.66
Quartz	2650	0.1	700	8.09

[1] Clark (1966)
[2] Berman & Brown (1985)

bles the underlying bedrock and consists mainly of dolomite (80%) and quartz, with varying amounts of feldspars and mica (Etzelmüller & Sollid 1991). The gravel (particles 0.5 to 5 cm in diameter), which is abundant even in the fine-grained soils, is dominantly comprised of carbonates (up to 83%). The Carbonates are mostly dolomite with some calcite (Mann et al. 1986). In this work the following representative mineralogy is used for the soil: 80% dolomite, 10% calcite and 10% quartz by volume.

The mean depth of the regolith at the field site is estimated to be 1.4 ± 0.2 m, based on hand-probing at the site in the late summer and examination of the soil stratigraphy at representative cross sections along the nearby Kvadehukelva (Kvadehukelva in Fig. 2). The cross sections revealed relatively thick regolith (Fig. 4) on major former beach ridges (Tolgensbakk & Sollid 1987) and thinner cover in swales between them. The field site is located in a swale between beach-ridges. The regolith thickness corresponds approximately with the active layer depth.

Porosity

Calculations of porosity are based on two sets of soil samples taken simultaneously from one excavation in sorted circle fines (8/6/85, S. Prestrud-Anderson). Samples were obtained from four different levels (0, 0.2, 0.4, and 0.6 m below surface) for bulk density and moisture content analyses (Fig. 5). For each level porosity was calculated from mean values of each data set. Uncertainty limits represent the combination of standard deviation of bulk density and moisture content. There appears to be a slight increase in porosity towards surface, but as it is well within uncertainty limits the whole section is assigned one representative porosity value: 0.26 ± 0.03. A few spot Time Domain Reflectometry (TDR)-measurements (Hydra Probe, Vitel Inc.) at the field site, when the soil was saturated, gave an average porosity of 0.29 ± 0.03 from the surface to a depth of 0.5 m. When uncertainties are taken into account, this corresponds well with the 0.26 value used throughout this work. The temporal evolution of soil moisture content is described below.

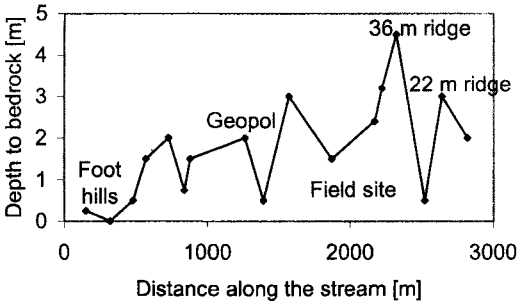

Fig. 4. Regolith thickness along the Kvadehukelva that cuts across elevated beach ridges near the field site. The thickness is greatest on beach ridges and thinnest in intervening swales. The field site is located in such a swale, where the regolith, as well as the active layer depth averages 1.4 ± 0.2 m in depth, based on late summer hand probing.

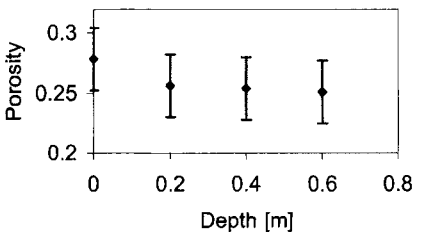

Fig. 5. Mean soil porosity as a function of depth, based on two sets of soil samples collected by S. Prestrud-Anderson on August 6, 1985, for bulk density and moisture content analyses. Uncertainty limits represent extreme combinations of bulk density and moisture content (each within one standard deviation of the mean).

Density

The soil bulk density is dictated by the porosity, moisture content and densities of constituent minerals (Table 1). The average of the mineral densities, weighted according to their volume fractions, is 2800 kg m^{-3}. The corresponding bulk densities of dry and water-saturated soil are 2070 kg m^{-3} and 2330 kg m^{-3}, using a porosity of 0.26.

Soil Moisture Content

The field site is located a few tens of metres from a small lake on an essentially horizontal surface and hence remains moist throughout the summer. A pore pressure transducer that reflects the height of the free water column was installed 0.55 m below the soil surface within the saturated soil domain. Depth to ground water table was also measured in a ground water tube, inserted 10 m from the site. These point measurements are generally consistent with the continuous pore pressure data. During most of July and August 1991, the ground water table depth was fairly stable, varying only within the vertical resolution of the thermal model. Therefore a representative mean value 0.4 m was applied in the corresponding thermal model.

Above the ground water table the fine-grained soil is unsaturated but still contains considerable capillary water. The unsaturated soil moisture content at the level of 0.2 m below surface was obtained by sampling the site weekly through the thaw season and determining the volumetric moisture content in the lab. The mean for the summer was 0.21 (σ = 0.02). This unsaturated soil moisture content is close to the expected value based on the soil moisture retention capacity that is estimated from the soil particle size distribution and the distance to water table (van Genuchten 1976). In conclusion, the soil moisture content at this study site does not vary appreciably during the course of the summer after the initial thaw at the beginning of July (Fig. 6).

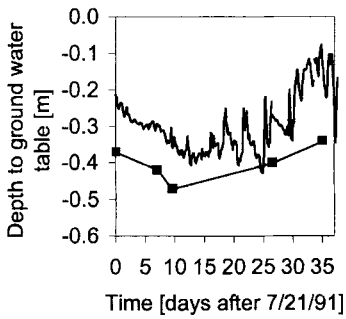

Fig. 6. Position of ground water table from pore pressure transducer and manual probing. The probed depth is measured about 10 m away and upslope from pore pressure transducer, which may account for the difference between data sets. In the model, the mean depth of 0.4 m was used from the end of July through August 1991.

Heat Capacity

The heat capacity of the mineral phase is 800.5 J kg^{-1} K^{-1}, based on the heat capacity of the primary minerals and their mass fractions (Berman & Brown 1985) (Table 1). The corresponding bulk soil volumetric heat capacities (ρc) range from $2.72 \cdot 10^6$ J m^{-3} K^{-1} for saturated soils to $1.68 \cdot 10^6$ J m^{-3} K^{-1} for dry soils. The heat capacity in the summer modeling reflects the observed soil moisture content.

For the winter period there are no independent measurements of the frozen soil heat capacities and of the distribution of ice, voids and mineral material. However, as the ratio of the heat capacities of ice to mineral matter is close to unity (0.93), the heat capacity is insensitive to variation in ice or mineral fraction. In contrast, in summer the corresponding ratio of water to mineral matter is 1.87. Consequently, in winter the heat capacity for the entire soil profile is assigned one representative value $2.1 \cdot 10^6$ J m^{-3} K^{-1}. The heat capacities of mineral material ($2.24 \cdot 10^6$ J m^{-3} K^{-1}) and ice ($2.1 \cdot 10^6$ J m^{-3} K^{-1}) are both within 7% of the suggested mean value. A small volumetric fraction of voids ($\sim$6%) in the soil will reduce the heat capacity to $\sim 2.1 \cdot 10^6$ J m^{-3} K^{-1}.

Thermal Conductivity

The thermal conductivity of the mineral fraction can be estimated closely (Sass et al. 1971) from the geometric mean of the conductivities of the individual mineral constituents (see Table 1):

$$k_{\text{solid}} = (k_{\text{Dolomite}})^{0.8}(k_{\text{Calcite}})^{0.1}(k_{\text{Quartz}})^{0.1} = 5.0\,\text{W m}^{-1}\,\text{K}^{1} \quad (2)$$

The thermal conductivity of near-surface (0.1 m depth) unsaturated soil was also measured by a

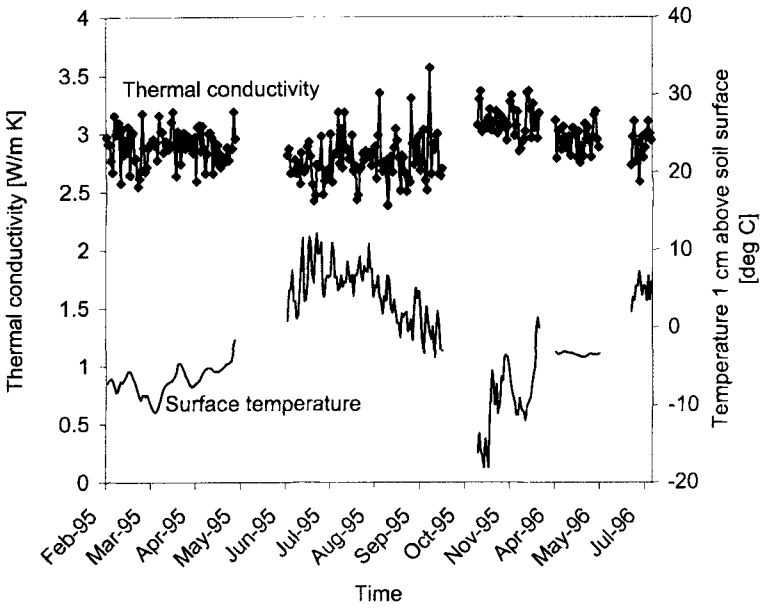

Fig. 7. In situ near surface (0.1 m) soil thermal conductivity measured with a needle probe, and temperature during the winter 1995 and summer 1996; note discontinuous time scale. The mean thermal conductivities for unfrozen and frozen soil for this period are respectively 2.8 W m^{-1} K^{-1} and 3.0 W m^{-1} K^{-1}. These differ significantly from laboratory measurements suggesting that the soil structure in remolded laboratory samples differs substantially from that in the field.

needle probe (Shiozawa & Campbell 1990), activated once a day to provide an in situ measurement during the 2/26/95–7/21/96 period (Fig. 7). The probe heats the soil for a short time period and simultaneously monitors the transient temperature, which is a function of thermal conductivity of the surrounding material (Shiozawa & Campbell 1990). The mean unfrozen and frozen thermal conductivities for this period are respectively 2.8 W m^{-1} K^{-1} and 3.0 W m^{-1} K^{-1}. Standard deviations are respectively 0.19 W m^{-1} K^{-1} (6.9%) and 0.16 W m^{-1} K^{-1} (5.6%), which correspond well with the reported (±5%) accuracy of the probe (Shiozawa & Campbell 1990). The measurements of the thermal conductivity of unfrozen soil compare favorably with 2.7 W m^{-1} K^{-1} value (0.26 porosity and 0.21 moisture content), calculated using an empirical relation suggested by Johansen (1975). Laboratory measurements with saturated soil sample from the field site yielded 2.7 W m^{-1} K^{-1} (σ = 0.04 W m^{-1} K^{-1}, 1.6%) for unfrozen soil (~20°C, porosity 0.30 ± 0.03) 3.9 W m^{-1} K^{-1} (σ = 0.32 W m^{-1} K^{-1}, 8.2%) for frozen soil at −15°C (Fig. 8). Similar measurements with a field site sample by M. Fukuda (pers. comm. 1993) yielded values for saturated sample: −20°C, 4.5 W m^{-1} K^{-1} and 20°C, 2.6 W m^{-1} K^{-1}, which generally agree with other data presented here. These numbers are similar to the geometric mean (equation 2) of respective conductivities of saturated soil (frozen 4.0 W m^{-1} K^{-1} and unfrozen 2.8 W m^{-1} K^{-1}). However, the field measurements are deemed most representative because the lab samples may have unrealistic soil structure and ice lens characteristics, which can affect the conductivity considerably (Hallet & Rasmussen 1993). The large difference between laboratory and in situ measured thermal conductivity for frozen soil suggests that in situ frozen soil near the ground surface contains air voids, lowering the thermal conductivity there. These voids are presumably formed in close connection with pervasive ice lensing within the soil structure (Hallet & Rasmussen, 1993).

The soil thermal conductivity was determined from temperature data for 0.1 m depth for the winter 1985/86 frozen ground because no direct thermal conductivity measurements were available for the period and location of interest. This was accomplished by using a thermal model based

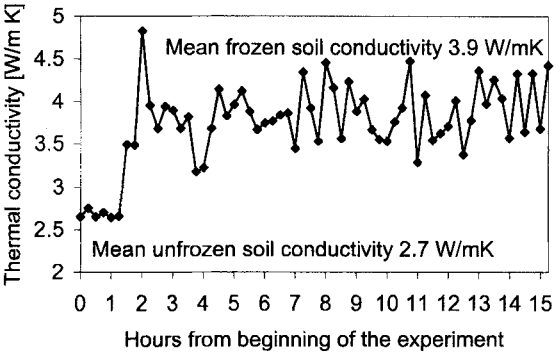

Fig. 8. Laboratory measurements of thermal conductivity of a saturated fine grained soil sample from the field site yielded average 2.7 W m^{-1} K^{-1} (standard deviation: 0.04 W m^{-1} K^{-1}) in the unfrozen (~20°C, porosity 0.30 ± 0.03) and 3.9 W m^{-1} K^{-1} (−15°C, standard deviation: 0.32 W m^{-1} K^{-1}) in the frozen state. The frozen 10^3 cm^3 sample was completely frozen in one hour. The rapid freezing and observed lack of ice lensing are probably responsible for the conductivity of the frozen sample being considerably higher than that measured in situ (Fig. 6).

on equation (1) and observed soil temperatures at two different levels within the uppermost 0.2 m as boundary conditions. The thermal conductivity was allowed to vary in order to find the effective thermal conductivity (2.0 W m^{-1} K^{-1}) that best reproduced the observed temperatures in the level between the two boundary temperatures.

It is expected that the conductivity varies with depth due to vertical variation in moisture content or textural characteristics. To determine if this is indeed the case, I examined periods when the time rate of temperature change at each model grid level vanishes ($dT/dt = 0$) in equation (1). For the temperature to stabilise, the divergence of the heat flux also has to vanish, which implies that

$$k_1\left(\frac{\partial T}{\partial z}\right)_1 = k_2\left(\frac{\partial T}{\partial z}\right)_2 \qquad (3)$$

where k_1 and k_2 are the thermal conductivities [W m^{-1} K^{-1}] of upper and lower control volumes respectively.

Thus (3) can be solved for the ratio of conductivities, and a complete conductivity profile can be obtained based on the independently measured surface conductivity (Fig. 9). A twofold increase in the thermal conductivity occurs between the surface and 1.2 m depth, presumably due to a decrease in void fraction and changes in texture and ice content with depth.

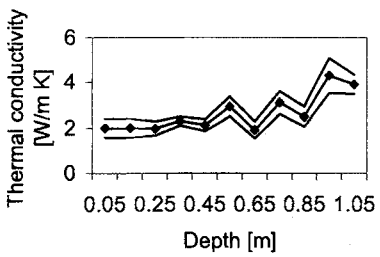

Fig. 9. Vertical thermal conductivity profile for the winter obtained from the temperature data (see text). Uncertainty limits of one standard deviation are also shown.

The conductivity profile is defined for a period with no rain-on-snow events and when soil temperatures were sufficiently low (~−10°C) to prevent complications caused by unfrozen water (as discussed below). This period was also chosen to include only temperature changes that were slow. If the soil temperatures were fluctuating rapidly, periods of vanishing dT/dt (as required when using equation 3) would be rare and short-lived, and the intermittent sampling could miss temperature peaks and hence misrepresent the mean thermal forcing during that period.

This method of determining the soil vertical conductivity profile is based on the following two assumptions: (1) conduction is the primary heat transfer process in the soil during this period, and no latent heat effects are present (for justification see section on soil internal evaporation); (2) heat flow is strictly one-dimensional and in the vertical direction. Failure of these assumptions would undermine the calculated conductivities. Additional errors could arise from the finite accuracy of the soil temperature measurements; however, these are likely to be minor because the typical temperature difference between adjacent thermistors is about an order of magnitude larger than the accuracy of the system (0.02°C).

Heat transfer processes in soil

Previous studies of the thermal behaviour of arctic soils have suggested that vapor advection and associated latent heat effects may significantly

contribute to the heat transfer in unfrozen soils (Hinkel & Outcalt 1993). Therefore, I have examined the heat transfer through both general calculations based on widely accepted theory on soil mass and energy flow (Philip & de Vries 1957) and thermal modeling based on field measurements of soil temperatures.

Advection of heat due to water motion

In addition to heat conduction, which always occurs when the temperature gradient and conductivity are both finite, heat advection due to pore fluid migration can be significant. Thermal effects of fluid flow in porous medium can be assessed by calculating the Peclet number that is a ratio between advective and conductive heat transfer (equation 4). To maximise advection effects, the most rapid flow velocity likely to occur naturally in the soil from the study site has been considered: the vertical velocity in a freely draining saturated soil. This water velocity ($u = 1.35 \cdot 10^{-8}$ m s^{-1}) was determined from the hydraulic conductivity obtained by centrifuge method (J. Conca pers. comm. 1993). Any rapid water flow is likely to be confined to the active layer, hence the active layer depth (~ 1.5 m) can be used for the characteristic length in the Peclet number:

$$Pe = \frac{uL}{\kappa} = 6.7 \cdot 10^{-3} \qquad (4)$$

where κ is representative bulk soil thermal diffusivity = $1 \cdot 10^{-6}$ m^2 s^{-1}.

The Peclet number ($2 \cdot 10^{-2}$) is much less than one, which suggests that heat advection due to water flow is negligible. Similar results have been reported from Taimyr, Siberia (Boike 1997).

During freeze up, the volumetric expansion of water due to freezing as well as ice lensing tend to break the soil structure and reduce the hydraulic conductivity, allowing more rapid infiltration once the soil thaws. However, the frost-induced increase in soil hydraulic conductivity is generally less than an order of magnitude (Chamberlain & Gow 1979) and, hence, advection is still very likely to be unimportant because the Peclet number is still much less than unity.

Soil internal evaporation

The importance of internal evaporation and condensation in the active layer, which has been stressed by Hinkel et al. (1990), Hinkel & Outcalt (1993) and Hinkel & Outcalt (1994) can be assessed through the physically based coupled energy and mass transfer model, formulated originally by Philip & de Vries (1957), modified by Milly (1982, 1984) and applied more recently by Scanlon & Milly (1994).

Vapor flux is governed by two relations:

$$q_{thermal\ vapor} = D_{thermal\ vapor} \frac{dT}{dz}$$

and

$$q_{isothermal\ vapor} = D_{isothermal\ vapor} \frac{d\psi}{dz}$$

Where: $q_{thermal\ vapor}$ is mass flux of vapor due to a thermal gradient [ms^{-1}], $D_{thermal\ vapor}$ is vapor conductivity associated with a temperature gradient [m^2 s^{-1} K^{-1}], $q_{isothermal\ vapor}$ is mass flux of vapor due to a pressure head gradient [m s^{-1}], $D_{isothermal\ vapor}$ is isothermal vapor conductivity [m s^{-1}], ψ is pressure head [m].

Both conductivities depend on temperature, soil moisture content and grain size distribution. To obtain a liberal order of magnitude estimate of the vapor flux, a soil temperature of 25°C is assumed (actual soils are colder and hence would have lower conductivities). In terms of soil moisture content, both conductivities peak in relatively dry soil. The highest conductivities found by Scanlon & Milly (1994) for two soils of interest (silty clay and loamy sand, which are similar to the study site soil, silt loam being slightly finer and the other slightly coarser) are $D_{thermal\ vapor} = -3 \cdot 10^{-11}$ m^2 s^{-1} K^{-1} and $D_{isothermal\ vapor} = 1 \cdot 10^{-14}$ m s^{-1}. The corresponding maximal vapor flux is

$$q_{thermal\ vapor} = -3 \cdot 10^{-11} \text{ m}^2 \text{ s}^{-1} \text{ K}^{-1} \ (dT/dz)$$

and corresponding latent heat flux in soil is

$$q_{thermal\ vapor}\ \rho_{water}\ L_e(dT/dz) = 0.075 \text{ W m}^{-1} \text{ K}^{-1} \ (dT/dz)$$

where: L_e is energy of evaporation = $2.5 \cdot 10^6$ J kg^{-1}. This vapor flux is directed from warm to colder domains. The maximum potential heat transfer contribution of thermal vapor flux is equivalent to an effective 3% increase in characteristic thermal conductivity (3 W m^{-1} K^{-1}).

The maximum isothermal vapor flux due to a pressure head gradient is calculated using the

$D_{isothermal\ vapor}$ ($1{\cdot}10^{-14}$ m s^{-1}) and the maximum assumed pressure head gradient. The pressure head of very fine grained surface soil is on the order of $-1.5{\cdot}10^{6}$ Pa (R. Sletten pers. comm. 1996), with water-saturated soil at 1 m depth and with such dry soil at the surface the pressure head gradient would be only 150 which is less than liberal order of magnitude estimate (10^{3}) used here for pressure head gradient:

$$q_{isothermal\ vapor} = 1 \cdot 10^{-14}\ m\ s^{-1}$$
$$10^{3} = 1 \cdot 10^{-11}\ \mathrm{m\ s^{-1}}$$

The corresponding latent heat transfer to the site of evaporation is

$$q_{isothermal\ vapor}\ \rho_{water}\ L_e = 1 \cdot 10^{-11}\ \mathrm{m\ s^{-1}}$$
$$10^{3}\ \mathrm{kg\ m^{-3}}\ 2.5 \cdot 10^{6}\ \mathrm{J\ kg^{-1}} = 0.025\ \mathrm{W\ m^{-2}}$$

Typical conductive soil heat fluxes exceed this latent heat transfer associated with vapor transport and condensation by more than two orders of magnitude; hence, thermal behaviour is for all practical purposes purely conductive. Other potential mechanisms to drive significant heat transfer in soil, such as chemically induced free energy gradients (Hinkel & Outcalt 1994), have yet to be documented.

Conduction with phase change, thermal conductivity gradient and unfrozen water

This section introduces processes and phenomena that figure importantly in but complicate the soil thermal analysis. These are commonly omitted from soil thermal models.

Thermal properties of natural soils vary vertically due to changes in texture, lithology, moisture and/or organic content (Woo & Xia 1996). The general thermal conduction equation (1) contains a term explicitly accounting for the thermal conductivity gradient. For many natural soils this conductivity gradient term turns out to be important. If omitted, non-conductive processes would need to be invoked to explain the thermal data. To assess the importance of the thermal conductivity gradient to the soil thermal regime, a representative period of early winter data (11/26–12/26/85) was analysed. The least squared error between observed and modeled soil temperatures for this period using the formerly determined soil conductivity gradient (see section on Thermal conductivity) is 0.15°C for the 1.1 m deep reference volume. The same calculation

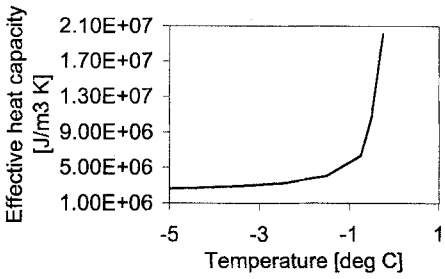

Fig. 10. Effective heat capacity reflecting the influence of the unfrozen water freezing at temperatures below 0°C. For this soil, practically all of the water freezes above −3°C (based on NMR measurements of unfrozen water in samples from the site by A. Tice, CRREL) rendering the effect of unfrozen water at lower temperatures negligible.

using the mean thermal conductivity reveals a least squared error of 0.48°C, 220% larger than optimal. Then, the least squared error was minimised, by finding the thermal conductivity constant over time and depth that produced the best fit between observed and modeled soil temperatures. This best fit mean thermal conductivity was 1.9 W m^{-1} K^{-1}, which is 32% smaller than the actual mean (2.8 W m^{-1} K^{-1}). Discrepancies are significant and suggest that the thermal conductivity gradient can be omitted only in cases of completely homogeneous soils, despite its common absence in soil thermal analyses.

Frozen soils are known to contain unfrozen water at temperatures well below 0°C (Williams & Smith 1989), which greatly increases the apparent heat capacity (requiring more energy to change the soil temperature) and lowers the thermal conductivity near 0°C (McGaw et al. 1978). For soil from this study site, most of the water freezes above −1°C. From −1°C to −3°C the apparent soil heat capacity is augmented by only about 10%, and below −3°C the contribution from unfrozen water is negligible (A. Tice pers. comm. Cold Regions Research and Engineering Laboratory (CRREL)) (Fig. 10). The unfrozen water that freezes at temperatures below 0°C dictates the typical gradual departure (approach) of temperatures from (to) 0°C (Fig. 11), which is characteristic of fine grained soils. Without this term, the modeled temperatures would depart abruptly from 0°C once all the water is frozen. The amount of unfrozen water content is soil specific, and omission of the term from models would lead to unrealistic results, particularly for fine-grained soils. Another well-known phenom-

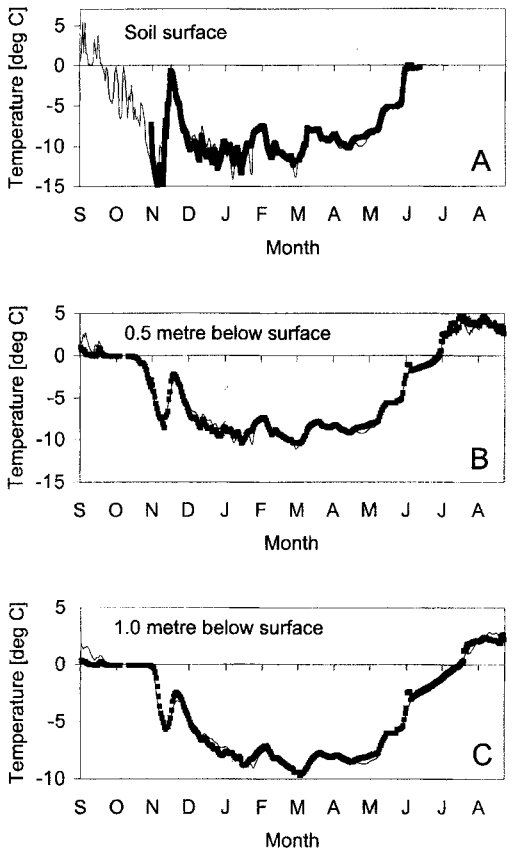

Fig. 11. Modeled (continuous line) and observed (squares) soil temperatures through one year at three levels in the soil: Surface (A), 0.5 metre below surface (B), and 1.0 metre below surface (C). Note the zero degree curtain that lasts over one month during the freeze up period due to the substantial amount of latent heat released as the bulk of the water freezes at 0°C and the typical gradual departure of temperatures from 0°C after the majority of the soil water has frozen up.

enon of freezing soils that is captured by the model is the formation of zero degree curtain, as the majority of the soil water freezes at a particular level, holding the soil temperatures at 0°C typically for many weeks.

The amount and location of ice growth and decay has considerable importance on soil thermal behaviour. To model soil temperatures correctly over freeze up and melt periods, the temperature data were used to solve for rates of formation and melting of ice as a function of time and depth (see details below).

Taking into account all these factors, which are generally disregarded in soil thermal models, the modeling accounted for much of the observed thermal behaviour and revealed reasonable values for thermal properties, closely resembling those measured in situ independently. There was generally no need to introduce non-conductive processes, except during the rapid warming events observed in the spring.

Characteristic soil thermal phases

Following is a summary of the primary characteristics of the soil thermal regime for thermally distinct periods of the year. The thermal field was modeled by making use of the observed soil surface temperature and heat flow, information on soil composition and thickness and on bedrock lithology, and assumed mean annual soil temperature 15 m below surface. The near surface soil thermal properties were solved by a one-dimensional standard heat transfer model (equation 1). Modeled temperatures from 0.1 m to 1.1 m depth (0.1 m increment) were compared to observed temperatures.

During the summer, conduction is the only significant heat transfer process. The propagation and attenuation with depth of the daily temperature signal is seen clearly in both modeled and observed soil temperatures (Fig. 10). The vertical variation in soil thermal conductivity necessitates the inclusion of the dk/dz-term in the general one-dimensional diffusion equation (Fig. 12).

Fall typically starts with persistently freezing air temperatures and light snowfall. The thermal regime is forced by sustained radiative energy loss at the ground surface resulting in slow conductive cooling in the soil. See Fig. (11) for modeled and observed soil temperatures during fall freeze up. Considerable latent heat is released as water

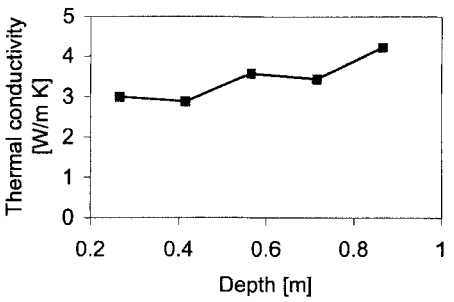

Fig. 12. Summer soil thermal conductivity profile. The 0.2 m conductivity was measured in situ, for conductivities at lower depths see the Fig. 6 caption for an explanation.

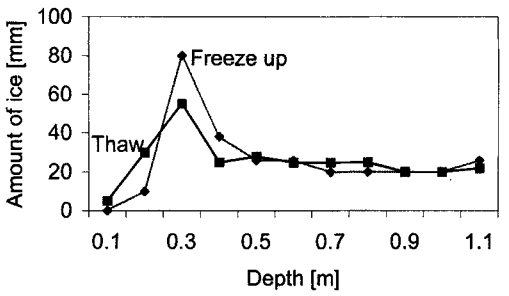

Fig. 13. Modeled amount of ice in the soil per depth increment formed during the 1985 fall freeze up and melted during the subsequent thaw period. Determined by allowing the ice amount in the model to evolve so that the correct timing of freeze up was reproduced at each level. The main modeled concentration of ice occurred 0.3 m below the ground surface. The total amount of ice thawed throughout the soil in the subsequent spring is within 2% of the calculated amount formed in the fall; however, the peak value at 0.3 m level is less pronounced during the spring presumably due to moisture redistribution during the snow cover period.

freezes, establishing the widely recognised zero-degree curtain in the active layer. Soil thermal properties change progressively during this period as a result of extensive water transfer and phase change that is manifested in considerable frost heaving. The soil moisture content and the amount of ice growth dictate the magnitude of latent heat effects. In the model, both the freezing of much of the water at 0°C and the progressive freezing of the remaining water at lower temperatures were taken into account through the latent heat term in equation (1).

The amount of ice that formed in the soil profile was determined by trial and error by allowing the ice amount in the model to evolve so that the correct timing of freeze up (temperature departure from 0°C) was reproduced at each level. Essentially all the heat is lost through the soil surface, hence the upper soil layers freeze first. Modeling the progressive descent of the freezing front, defined as the 0°C isotherm, makes it possible to calculate the amount of ice that forms as a function of time and depth. According to the model, the maximum ice concentration occurred 0.3 ± 0.05 m below the surface (Fig. 13). No ice lensing took place near the surface, probably because the surface soil froze faster than it could draw water from below. This appears to contradict soil surface heave records from other years that show that considerable soil expansion occurs due to ice growth within 0.2 m of the ground surface. This discord may arise from the summer before the observation period having been extremely dry. During July–September 1985, the precipitation was 33.2 mm which is the lowest in the existing data set (1983–1991) and less than 38% of the average for the same period. This suggests that the ground was drier than usual, inhibiting the near surface ice growth.

The total amount of ice that formed within the active layer was 296 mm of water equivalents, which is close to the suggested saturated water content for the same thickness. Moreover, the ice content profile obtained for the fall freeze-up is entirely consistent with the one deduced for the subsequent spring thaw (Fig. 13), which adds support for both. In conclusion, the model seems to capture the thermal behaviour observed in the field, and hence the evolution of active layer soil temperatures during fall freeze up can be modeled by conduction with phase change.

Winter soil temperatures (Fig. 11) are also generally dictated by conduction. During late spring (May–June), when considerable heat is provided by the sun to melt snow, the comparison of modeled and observed soil temperatures are suggestive of non-conductive events, probably moisture percolation into the frozen soil causing rapid warming as latent heat is released by freezing water. An independent heave record shows heave activity during the same period (May/11 and June/2/86), which lends further merit to this suggestion. During this period the 1.1 m thick soil layer warmed an average of 6°C, only 47% of which appears to be due to conductive heating. In the model, the soil temperatures were allowed to closely follow the observations. This required a non-conductive warming within the soil profile. Assuming that the warming is due to water percolating in the ground and freezing there, the amount of water that froze can be calculated. The heat liberated by the freezing of 35 mm of water could account for this warming.

To determine the amount of ice in the soil profile during spring melt, the ice concentration in the model was adjusted to reproduce the correct timing of the onset of thawing at each reference level. The amount of ice needed to satisfy the conductive model during the melt period was then compared to the amount of ice that was produced during the previous fall. The total amount of ice that formed during fall and the separately calculated amount that melted during the spring within the whole reference volume are within 2% of each other. The ice content variation with depth

is similar, but the peak value at 0.3 m level is less during spring melt (for ice content see Fig. 13, and for modeled and observed soil temperatures see Fig. 11). This can partly be explained by the percolation of water from thawed soil into the still frozen soil near 0°C, and the related advective transfer of heat, as shown by Mackay (1983).

Conclusions

The thermal link between the atmosphere and the permafrost is central to interpreting climate change records contained in permafrost temperatures and to predicting climate change consequences in high-latitude and high-altitude areas. This link was studied by examining the heat transfer processes that dictate soil temperatures and heat flow for an arctic desert site in western Spitsbergen (78°57′29N, 12°27′42E).

The modeling of the soil thermal regime requires a precise determination of soil thermal properties and soil heat transfer processes. Although it is common practice to assign constant representative thermal properties to soils of interest, the thermal properties of natural soils tend to vary spatially due to changes in texture, lithology, moisture and/or organic content, and they vary with time primarily due to changes in moisture and in the relative amounts of ice and water. The one dimensional thermal conduction equation (1) contains a term explicitly accounting for the vertical thermal conductivity gradient, which is important in the energy balance for the soil at the study site and, by inference, for other natural soils. If it is omitted, it leads to an apparent need to invoke processes other than conduction or thermal properties that are unrealistic. Accurate thermal modeling for laterally homogeneous soils on sub-horizontal surfaces requires in situ observations of vertically and temporally varying soil thermal properties; if thermal properties varied laterally, accurate thermal modeling would require inclusion of the complete three-dimensional spatial variation of the thermal parameters, as well as variations in surface and other significant properties (vegetation, albedo, texture, moisture).

Water that remains unfrozen in soils at subzero temperatures, which is often neglected in soil thermal models, is important for realistic modeling of soil temperatures at the field site. During the freeze up (thaw) period, the unfrozen water dictates the typical gradual departure (approach) of temperatures from (to) 0°C. Without this term, modeled temperatures would depart abruptly from 0°C once all the water is frozen. Below approximately −3°C, the effect of unfrozen water increasing the apparent heat capacity and lowering of thermal conductivity of the soil at the field site (McGaw et al. 1978) is practically negligible.

Thermal conduction is the only significant heat transfer process at this site in the soil during the summer and most of the winter. Other heat transfer processes have been invoked in other areas, but they seem unimportant in western Spitsbergen. In addition, theoretical considerations indicate that coupled energy and mass transfers contribute only insignificantly to the soil energy budget. Comparisons between modeled and observed soil temperatures are suggestive of distinct periods in the late spring when water that has become abundant in the snow percolates into and rapidly warms the frozen soil. This form of latent heat transfer amounts to 53% of the total energy delivered to the soil during these warming periods; the rest is primarily due to heat conduction.

Acknowledgements. – The author wishes to express sincere appreciation to the following professors who contributed to this work by serving as members of author's Ph.D. advisory committee: chairman B. Hallet, E. Waddington, L. Fritschen, L. Washburn, and S. Warren. The dissertation was reviewed by B. Hallet, E. Waddington, and L. Washburn who substantially improved the presentation. The author also wants to express gratitude to W. Haeberli and an anonymous reviewer for suggestions for improving the manuscript.

The following individuals contributed to making this work possible: P. Berg, T. Berg and H. Conway; other support was given by G. Aasebøstøl, T. I. Karlsen and S. Thon from the Norwegian Polar Institute, B. Aune and I. Hanssen-Bauer from the Norwegian Meteorological Institute and M. Fukuda, J. Conca, D. McTique and B. Bruner.

The following institutions helped by their co-operation and generous offers to use their infrastructure; The Norwegian Polar Institute, the Norwegian Meteorological Institute, Kings Bay Coal Company in Ny-Ålesund and Velferden which allowed the use of the Geopol-hut. The work was funded by the Academy of Finland, the National Science Foundation (USA) and the US Army Research Office.

References

Bejan, A. 1993: *Heat transfer*. J. Wiley & Sons, Inc. 675 pp.

Berman, R. G. & Brown, T. H. 1985: Heat Capacity of Minerals in the System Na_2O-K_2O-CaO-MgO-FeO-Fe_2O_3-

Al_2O_3-SiO_2-TiO_2-H_2O-CO_2: Representation, Estimation, and High0 Temperature Extrapolation. *Contrib. Mineral. Petrol. 89*, 168–183.

Boike, J. 1997: Thermal, hydrological and geochemical dynamics of the active layer at a continuous permafrost site, Taymyr Peninsula, Siberia. *Reports on Polar Research, Vol. 242, 1997.* Alfred Wegener Institute for Polar and Marine Research, Bremerhaven, Germany.

Budyko, M. I. & Izrael, Y. A. 1987: *Anthropogenic Climatic Change*. Hydrometeoizdat, Leningrad (in Russian; English ed. published by the University of Arizona Press 1992). 405 pp.

Chamberlain, E. D. & Gow, A. J. 1979: Effect of Freezing and Thawing on the Permeability and Structure of Soils. Pp. 73–92 in Jessberger, H. L. (ed.): Ground Freezing. *Eng. Geol. 13(1–4)*.

Clark, S. P. 1966: *Thermal conductivity in Handbook of Physical Constants: Memoir 97*. S. P. Clark, editor. Geological Society of America, New York. Pp. 459–482.

Etzelmüller, B. & Sollid, J. L. 1991: The role of weathering and pedological processes for the development of sorted circles on Kvadehuksletta, Svalbard – a short report. *Polar Res. 9(2)*, 181–191.

Goodrich, L. E. 1982: The Influence of Snow Cover on the Ground Thermal Regime. *Can. Geotech. J. 19*, 421–432.

Gregersen, O. & Eidsmoen, T. 1988: *Permafrost Conditions in the Shore Area at Svalbard.* Fifth International Conference on Permafrost in Trondheim, Norway, August 1988. Vol. 2. Pp. 933–936.

Hallet, B. & Prestrud, S. 1986: Dynamics of Periglacial Sorted Circles in Western Spitsbergen. *Quat. Res. 26*, 81–99.

Hallet, B. & Rasmussen, A. 1993: *Calculation of the Thermal Conductivity of Unsaturated Frozen Soil near the Melting Point*. Permafrost Sixth International Conference Proceedings. Vol. 1. Pp. 226–231. South China University of Technology Press.

Hinkel, K. M. & Outcalt, S. I. 1993: Detection of Nonconductive Heat Transport in Soils Using Spectral Analysis. *Water Resour. Res. 29(4)*, 1017–1023.

Hinkel, K. M. & Outcalt, S. I. 1994: Identification of Heat-Transfer Processes during Soil Cooling, Freezing and Thaw in Central Alaska. *Permafrost Periglacial Proc. 5*, 217–235.

Hinkel, K. M., Outcalt, S. I. & Nelson, F. E. 1990: Temperature Variation and Apparent Thermal Diffusivity in the Refreezing Active Layer, Toolik Lake, Alaska. *Permafrost Periglacial Proc. 1*, 265–274.

IPCC. 1996: (Intergovernmental Panel on Climate Change). Climate Change 1995, The Science of Climate Change. Cambridge University Press. 572 pp.

Judge, A. & Pilon, J. 1983: *Climate Change and Geothermal Regime*. Introduction in Fourth International Conference on Permafrost, Final Proceedings, National Academy Press, US. Pp. 137–138.

Kahl, J. D., Charlevoix, D. J., Zaitseva, N. A., Schnell, R. C. & Serreze, M. C. 1993: Absence of Evidence for Greenhouse Warming over the arctic Ocean in the Past 40 Years. *Nature 361(6410)*, 335–337.

Kane, D. L., Hinzman, L. D. & Zarling, J. P. 1991: Thermal Response of the Active Layer to Climatic Warming in a Permafrost Environment. *Cold Regions Sci. Tech. 19(2)*, 111–122.

Lachenbruch, A. H. & Marshall, B. V. 1986: Changing Climate: Geothermal Evidence from Permafrost in the Alaskan Arctic. *Science 234*, 689–696.

Liestøl, O. 1975: Glaciological Work in 1972. *Norsk Polarinst. Årbok* 1972, 125–135.

Løvlie, R. & Putkonen, J. 1996: Dating of thaw depths in permafrost terrain by the palaeomagnetic method: experimental acquisition of a freezing remanent magnetization. *Geophys. J. Int. 125*, 850–856.

Mackay, J. R. 1983: Downward water movement into frozen ground, western arctic coast, Canada. *Can. J. Earth Sci. 20(1)*, 120–134.

Mann, D. H., Sletten, R. S. & Ugolini, F. C. 1986: Soil Development at Kongsfjorden, Spitsbergen. *Polar Res. 4*, 1–16.

Maxwell, J. B. & Barrie, L. A. 1989: Atmospheric and Climatic Change in the Arctic and Antarctic. *Ambio 1*, 42–49.

McGaw, R. W., Outcalt, S. I. & Ng, E. 1978: *Thermal Properties and Regime of Wet Tundra Soils at Barrow, Alaska.* Third International Conference on Permafrost, Proceedings, Vol. 1. July 10–13, 1978, Edmonton, Alberta, Canada. National Research Council of Canada. 47 pp.

Meehl, G. A., Washington, W. M., Erickson III, D. J., Briegleb, B. P. & Jaumann, P. J. 1996: Climate Change from Increased CO_2 and Direct and Indirect Effects of Sulfate Aerosols. *Geophys. Res. Lett. 23(25)*, 3755–3758.

Milly, P. C. D. 1982: Moisture and Heat Transport in Hysteretic, Inhomogeneous Porous Media: A Matric Head-Based Formulation and a Numerical Model. *Water Res. Res. 18(3), 489–498.*

Milly, P. C. D. 1984: A Simulation Analysis of Thermal Effects on Evaporation From Soil. *Water Res. Res. 20(8)*, 1087–1098.

Nelson. F. E. & Anisimov, O. A. 1993: Permafrost Zonation in Russia under Anthropogenic Climatic Change. *Permafrost Periglacial Proc. 4(3)*, 137–148.

Nelson, F. E., Lachenbruch, A. H., Woo, M.-K., Koster, E. A., Osterkamp, T. E., Gavrilova, M. K. & Guodong, C. 1993: *Permafrost and Changing Climate*. Sixth International Conference on Permafrost. South China University of Technology, Wushan Guangzhou, China. Presentation by authors in plenary session on 'Global Climate Change and Permafrost'.

Oechel, W. C., Hastings, S. J., Vourlitis, G. V., Jenkins, Riechers, M. G. & Grulke, N. 1993: Recent Change of Arctic Tundra Ecosystems from a Net Carbon Dioxide Sink to a Source. *Nature 361*, 520–523.

Osterkamp, T. E. & Gosink, J. P. 1991: Variations in Permafrost Thickness in Response to Changes in Paleoclimate. *J. Geophys. Res. 96(B3)*, 4423–4434.

Ozisik, M. N. 1968: *Boundary Value Problems of Heat Conduction*. Dover Publications, Inc. 504 pp.

Philip, J. R. & de Vries, D. A. 1957: Moisture Movement in Porous Materials under Temperature Gradients. *Trans. Am. Geophys. Union 38(2)*, 222–232.

Putkonen, J. K. in press: Suitability Of Central Alaska For Early Detection Of Climate Warming. International Permafrost Association 7th Conference, Yellowknife.

Richtmeyer, R. D. & Morton, K. W. 1967: Difference Methods for Initial Value Problems. J. Wiley & Sons.

Riseborough, D. W. & Smith, M. W. 1993: Modeling Permafrost Response to Climate Change and Climate Variability. Pp. 179–187 in Lunardini, V. J. & Brown, S. L. (eds.): *Proceedings, Fourth International Symposium on Thermal Engineering & Science for Cold Regions*. US Army Cold Regions Research and Engineering Laboratory, Special Report 93-22. Hanover, NH.

Romanovsky, V. E. & Osterkamp, T. E. 1995: Interannual Variations of the Thermal Regime of the Active Layer and Near-Surface Permafrost in Northern Alaska. *Permafrost Periglacial Proc. 6*, 313–335.

Roots, E. F. 1989: Climate Change: High Latitude Regions. *Climatic Change 15(1/2)*, 223–253.

Salvigsen, O. & Mangerud, J. 1991. Holocene shoreline displacement at Agardhbukta, eastern Spitsbergen, Svalbard. *Polar Res. 9(1)*, 1–7.

Santer, B. D., Taylor, K. E., Wigley, T. M. L., Penner, J. E., Jones, P. D. & Cubasch, U. 1995: Towards the Detection and Attribution of an Anthropogenic Effect on Climate. *Climate Dynamics 12*, 77–100.

Sass, J. H., Lachenbruch, A. H. & Munroe, R. J. 1971: Thermal Conductivity of Rocks from Measurements of Fragments and Its Application to Heat-Flow Determinations. *J. Geophys. Res. 76(14)*, 3391–3401.

Scanlon, B. R. & Milly, P. C. D. 1994: Water and Heat Fluxes in Desert Soils 2. Numerical Simulations. *Water Resour. Res. 30(3)*, 721–733.

Shiozawa, S. & Campbell, G. S. 1990: Soil Thermal Conductivity. *Remote Sensing Rev. 5(1)*, 301–310.

Sturm, M., Holmgren, J. & Liston, G. E. 1995: A Seasonal Snow Cover Classification System for Local to Global Applications. *J. Climate 8(5)*, 1261–1283.

Tolgensbakk, J. & Sollid, J. L. 1987: Geomorphology and Quaternary geology of Kvadehuksletta 1:10000. *Norsk Polarinst. Temakart 8*, 1987.

van Genuchten, M. Th. 1976: A Closed Form Equation for Predicting the Hydraulic Conductivity of Unsaturated Soils. *Soil Sci. Soc. Am. J. 44*, 892–898.

Walsh, J. E. 1993: The Elusive Arctic Warming. *Nature* Vol. 361 (6410), pp. 300–301.

Weller, G. & Holmgren, B. 1974: The Microclimates of the Arctic Tundra. *J. Appl. Meteorol. 13*, 854–862.

Williams, P. J., & Smith, M. W. 1989: *The Frozen Earth, Fundamentals of Geocryology. Studies in Polar Research.* Cambridge University Press. 306 pp.

Woo, M. & Heron, R. 1981: Occurrence of Ice Layers at the Base of High Arctic Snowpacks. *Arct. Alp. Res. 13(2)*, 225–230.

Woo, M. & Xia, Z. 1996: Effects of Hydrology on the Thermal Conditions of the Active Layer. *Nordic Hydrol. 27*, 129–142.

Appendix A. Finite difference discretisation

A frequently used and readily applicable method in the numerical solution of differential equations is the finite-difference approximation of the partial derivatives (Ozisik 1968; Richtmeyer & Morton 1967; Bejan 1993). The one dimensional transient diffusion of heat is described by equation (A.1)

$$\rho c \frac{\partial T}{\partial t} = \frac{\partial}{\partial z}\left(k \frac{\partial T}{\partial z}\right) \tag{A.1}$$

where T is temperature [°C], t is time [s], ρc is heat capacity [J m^{-3} K^{-1}], k is thermal conductivity [W m^{-1} K^{-1}], z is depth [m].

The explicit forward discretisation of equation (A.1) is represented by equation (A.2)

$$\rho c \frac{T_i^{n+1} - T_i^n}{\Delta t} = \left[k_{i-1}\left(\frac{T_{i-1}^n - T_i^n}{\Delta x}\right) - k_i\left(\frac{T_i^n - T_{i+1}^n}{\Delta x}\right)\right]\frac{1}{\Delta x} \tag{A.2}$$

where n indicates the time step and i represents equally spaced nodes along the z-axis.

The solution will be numerically stable if (Ozisik 1968; Richtmeyer & Morton 1967):

$$\frac{\left(2\frac{k}{\rho c}\Delta t\right)}{(\Delta x)^2} \leq 1 \tag{A.3}$$

This essentially defines the mesh dimensions (length and time increments).